INTERNATIONAL JOURNAL FOR NUMERICAL METHODS IN FLUIDS
Int. J. Numer. Meth. Fluids 2004; **46**:983–1005
Published online 6 October 2004 in Wiley InterScience (www.interscience.wiley.com). DOI: 10.1002/fld.782

k–l based hybrid LES/RANS approach and its application to heat transfer simulation

Bowen Zhong[1] and Paul G. Tucker[2,*,†]

[1]*CFD Lab, Engineering Department, Cambridge University, Trumpington Street, Cambridge, CB2 1PZ, U.K.*
[2]*Civil and Computational Engineering Centre, School of Engineering, The University of Wales, Swansea, SA2 8PP, U.K.*

SUMMARY

To improve the compatibility of a k–l based hybrid LES/RANS approach, a controllable transitional zone is introduced to bridge the RANS and LES zones. This allows blending of the very different modelled turbulence length scales in these regions. To obtain a smooth variation of the length scales and transitional zone parameters different weighting functions are proposed. Results show the 'RANS' region has significant coherent unsteadiness. For Unsteady RANS (URANS) theoretical correctness, a favourable spectral gap between the modelled and resolved scales is required. The use of unsteadiness damping and time step filtering to ensure this is explored. Approaches are tested for a plane channel flow and the flow over a matrix of surface mounted cubes. The capability of the new hybrid LES/RANS method in improving heat transfer prediction in a conjugate heat transfer problem is examined. Numerical tests show that, compared to the RANS simulation, the proposed hybrid LES/RANS scheme performs well for the flow with large scale unsteadiness. It is also effective for improving the prediction of heat transfer. Copyright © 2004 John Wiley & Sons, Ltd.

KEY WORDS: hybrid LES/RANS; LES; k–l model; plane channel flow; surface mounted cube; heat transfer

1. INTRODUCTION

For the flows with large scale unsteadiness, large eddy simulation (LES) has proven more accurate than Reynolds averaged Navier–Stokes equations (RANS) simulations. However, LES places strong near wall grid demands. In order to resolve near wall streak like turbulent structures, LES requires that the grid spacings, in wall units, should be about $y^+ = 1$, $\Delta x^+ = 100$, $\Delta z^+ = 20$, in the wall normal, streamwise and spanwise directions, respectively [1]. This

*Correspondence to: P. G. Tucker, Civil and Computational Engineering Centre, School of Engineering, The University of Wales, Swansea, SA2 8PP, U.K.
†E-mail: P.G.Tucker@swansea.ac.uk

Contract/grant sponsor: Engineering and Physical Sciences Research Council (EPSRC); contract/grant number: GR/N39920/01

Received 16 November 2003
Revised 6 August 2004

becomes prohibitive for most high Reynolds number engineering problems. Spalart *et al.* [2] estimated that LES is unlikely to be used in aircraft design until the year 2045, even allowing for generous rate increases in computer speed.

To circumvent the LES expense, various near wall modelling methods have been considered [3]. One is the wall function approach [4–6]. This is similar to the high Reynolds number modelling approach used in RANS simulations. Others are the hybrid approaches developed more recently [5]. There are essentially three strategies available in this hybrid category, namely, the thin boundary layer (TBL) approach of Balaras *et al.* and Cabot and Moin [7, 8], the limited numerical scales (LNS) approach of Batten *et al.* [9–11] and zonal hybrid LES/RANS approaches [2, 12–20]. The TBL approach employs the thin layer form of the Reynolds averaged Navier–Stokes equations just within the near wall region. This provides an unsteady boundary condition to the LES region. The LNS approach, inspired by Speziale's work [21], determines the switch between the LES and RANS regions by scaling the eddy viscosity by a parameter α. This parameter is a function of turbulent length and velocity scales. For RANS $\alpha = 1$ and for LES $\alpha < 1$. The most well-known zonal hybrid LES/RANS method is the detached eddy simulation (DES) approach proposed by Spalart *et al.* in 1997 [2, 12, 13]. This makes use of the Spalart–Allmaras (S–A) model [22] in both the RANS and LES regions. The switch from RANS to LES, giving Spalart's approach its zonal nature, is determined by equating the nearest wall distance to a scaled LES characteristic filter width. The approach has been applied to simulate, for example, the process of dynamic stall of an airfoil, the vortex shedding behind a circular cylinder and flows around a highly complex three dimensional aircraft landing gear geometry [14]. Inspired by Spalart *et al*'s work, several hybrid LES/RANS approaches with different RANS and LES subgrid scale model combinations have been developed in the last few years. Typically, Davidson and Peng [15] combine a two equation near wall k–ω RANS model with a one-equation LES subgrid scale (SGS) model. In an *a priori* study, Temmerman *et al*. [16] couple a one-equation RANS k–l model with the Smagorinsky LES SGS model. Hamba [17] uses a k–ε near wall model with a one-equation LES SGS model. Tucker and Davidson [18] utilize the similarity of form of a RANS k–l model and the k–l based LES model of Yoshizawa [23] proposing a k–l based zonal LES approach. The interface length scales are smoothed using a multigrid related smoothing function. This approach has been applied to plane and ribbed channel flows. It is found effective at improving the predicted flow and heat transfer. Temmerman *et al*. [20] also investigate a k–l based hybrid RANS/LES approach, enforcing continuity in the total viscosity across the RANS/LES interface. Their approach is applied to a plane channel and a channel with a bump.

Although all the aforementioned research work shows that hybrid LES/RANS schemes are generally promising, there are still some fundamental issues that need to be resolved. These relate to, for example, the RANS and LES model compatibility, and resolved turbulence level arising from the interaction between the RANS and LES regions. For a plane channel flow, it is found that a smooth and accurate law of wall is difficult to obtain by using hybrid LES/RANS schemes. Since the motivation for this work is lower Reynolds number flows, the LES/RANS interface tends to be placed in the inner part of the logarithmic region. If the RANS/LES interface is placed in this region, excessive near wall resolved turbulence can arise. Having the interface further out can damp resolved motions away from walls.

In order to improve the compatibility of the k–l based hybrid LES/RANS approach proposed by Tucker and Davidson [18], in this paper, a controllable transitional zone is introduced to

bridge RANS and LES zones. Different weighting functions are proposed to obtain a smooth variation of the length scales and transitional zone parameters. Also, to improve predicted near wall resolved turbulence levels and ensure URANS theoretical correctness, the use of spatially adapted time steps and near wall velocity damping is explored. The new methods are tested and applied to a plane channel flow and that around a matrix of surface mounted cubes [24, 25]. Results are compared to measurements, LES data and the RANS solution of Rautaheimo and Siikonen [26].

2. NUMERICAL METHODS

2.1. Governing equations

Time averaged and filtered governing equations can be written in the same incompressible form, as follows:

$$\frac{\partial \tilde{u}_j}{\partial x_j} = 0 \tag{1}$$

$$\frac{\partial \tilde{u}_i}{\partial t} + \frac{\partial \tilde{u}_i \tilde{u}_j}{\partial x_j} = \frac{\delta_{1j}\beta}{\rho} - \frac{1}{\rho}\frac{\partial \tilde{p}}{\partial x_i} + \frac{1}{\rho}\frac{\partial}{\partial x_j}\left[(\mu + \mu_{\mathrm{T}})\frac{\partial \tilde{u}_i}{\partial x_j}\right] \tag{2}$$

$$\frac{\partial \tilde{T}}{\partial t} + \frac{\partial \tilde{T}\tilde{u}_j}{\partial x_j} = \frac{\alpha \tilde{u}_1}{\rho} + \frac{1}{\rho}\frac{\partial}{\partial x_j}\left[\left(\frac{\mu}{Pr} + \frac{\mu_T}{Pr_{\mathrm{T}}}\right)\frac{\partial \tilde{T}}{\partial x_j}\right] \tag{3}$$

The parameters α and β are mean temperature and pressure gradients. These are used to aid the implementation of the periodic streamwise boundary conditions [27, 28]. The tildes ($\sim$) used in Equations (1)–(3) denote that time averaging is applied in the RANS region and filtering in the LES. Consequently, in the RANS region the turbulent viscosity $\mu_{\mathrm{T}} = \mu_t$, the eddy viscosity. In the LES region $\mu_{\mathrm{T}} = \mu_{\mathrm{SGS}}$, the subgrid scale viscosity. The turbulent Prandtl number Pr_{T} used in the RANS and LES regions are 0.9 and 0.6, respectively.

In this paper, as in Reference [18], Wolfshtein's k–l RANS model [29] is employed to obtain the near wall eddy viscosity. The subgrid scale k_{SGS}–l LES model of Yoshizawa [23] and Fureby [30] is used away from walls. The RANS and SGS models are mathematically of the same form. Just some constants and the length scales definitions are changed. Both models can be written as follows:

$$\frac{\partial k_{\mathrm{T}}}{\partial t} + \frac{\partial \tilde{u}_j k_{\mathrm{T}}}{\partial x_j} = \frac{1}{\rho}\frac{\partial}{\partial x_j}\left[\left(\mu + \frac{\mu_{\mathrm{T}}}{\sigma_k}\right)\left(\frac{\partial k_{\mathrm{T}}}{\partial x_j}\right)\right] + P_{k_{\mathrm{T}}} - \varepsilon_{\mathrm{T}} \tag{4}$$

where $\sigma_k = 1$ is the diffusion Prandtl number for k and $P_{k_{\mathrm{T}}}$ is the turbulence production term. The subscript 'T' is used again here to identify whether a RANS or a SGS model is used. For all models, Equation (4) is solved with

$$\varepsilon_{\mathrm{T}} = C_\varepsilon k_{\mathrm{T}}^{3/2}/l_\varepsilon \tag{5}$$

and

$$\mu_{\mathrm{T}} = \rho C_\mu l_\mu k^{1/2} \tag{6}$$

The RANS constants used in Equations (5) and (6) are $C_\varepsilon = 1$ and $C_\mu = 0.09$. The RANS length scales used in Equations (5) and (6) are defined as

$$l_\varepsilon = 2.4y(1 - \mathrm{e}^{-0.263y^*}) \tag{7}$$

$$l_\mu = 2.4y(1 - \mathrm{e}^{-0.016y^*}) \tag{8}$$

where $y^* = y\rho k_{\mathrm{T}}^{1/2}/\mu$. For the LES region, as suggested by Fureby [30], the constants $C_\varepsilon = 1.05$ and $C_\mu = 0.07$. Also, l_ε and l_μ are replaced by the 'filter' size $(\Delta x \Delta y \Delta z)^{1/3}$. Without blending, incompatibilities between RANS and LES zones are to be expected.

2.2. *Hybrid LES/RANS approach*

Tucker and Davidson's zonal approach [18] combines a k–l one-equation RANS model with Yoshizawa's k_{sgs}–Δ subgrid LES model. The interface location method is a development of Davidson's earlier specified interface work [15]. The interface is fixed around the inner part of the logarithmic region. This gives a modelled turbulence length scale mismatch. Hence, the length scales at the interface are blended by a multigrid related smoothing function. This is different from Spalart's DES approach [2]. With this, the interface is taken as where the wall normal distance and the scaled filter size are equal, i.e. $y = 0.65\Delta$. Hence the RANS/LES interface in the Spalart's DES approach is purely grid controlled. In order to simulate a flow field properly, after an initial computation, the grid may need to be redistributed and even subsequently further refined. Otherwise, the RANS/LES interface may be too close to or too far away from the wall, leading to bad simulation results.

Here, as in Reference [18], the RANS/LES interface position is specified. In order to control the RANS/LES zone interaction, in a similar manner to Hamba [17], a transitional zone between the pure RANS and the LES regions is introduced. The transitional zone is defined as follows: If $y^+ \leqslant y_A^+$, RANS is used; if $y^+ \geqslant y_B^+$, LES is applied; otherwise, it is a transitional zone. For the transitional zone, weighting function based expressions are introduced for the length scales and constants. These are defined as follows:

$$l_{\mathrm{TRAN}} = (1 - s)l_{\mathrm{RANS}} + sl_{\mathrm{LES}} \tag{9}$$

$$c_{\mathrm{TRAN}} = (1 - s)c_{\mathrm{RANS}} + sc_{\mathrm{LES}} \tag{10}$$

where c represents modelling constants. The subscripts RANS, LES and TRAN in Equations (9) and (10) denote the values of the length scales and constants in the RANS, LES or transitional zone, respectively. The parameter s $(0 \leqslant s \leqslant 1)$ is a weighting function. If we define

$$\xi = (y^+ - y_A^+)/(y_B^+ - y_A^+) \tag{11}$$

and set $s = \xi$, then s becomes a linear weighting function. If s is set to 0 or 1, the transitional zone becomes a RANS zone with an interface at y_B^+ or a LES zone with an interface at y_A^+.

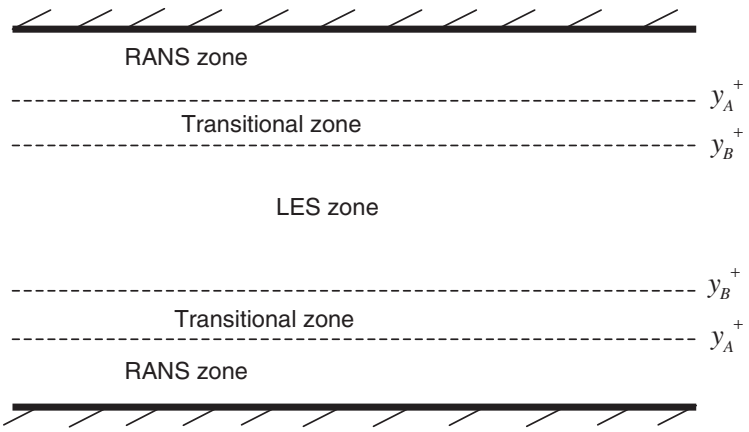

Figure 1. Locations of different modelling zones.

The following functions are tested:

$$s = \xi^n \tag{12a}$$

$$s = \sin^n(\pi\xi/2) \tag{12b}$$

where $n = 1/3, 1/2, 1, 2, 3$.

Since l in Equations (9) and (10) is spatially non-linear, it is obvious that the linear weighting function applied here is not simply a linear spatial interpolation between two interfaces. The advantage of the weighting function approach is that, it avoids the need to store the length scales and constants at the interfaces. The length scales l_{TRAN}, the constant c_{TRAN} and the weighting function s are evaluated locally by the local values of l_{RANS}, l_{LES}, c_{RANS}, c_{LES} and y^+. This saves computational effort and eases implementation. Figure 1 shows the locations of different modelling zones in a plane channel. A zone reminiscent of the so-called 'DES buffer/transitional layer' (Reference [3]) is created.

2.3. Solution for flow equations

In this paper, the pressure-correction based SIMPLE method is used for solving the governing equations. The Crank–Nicolson scheme in time and central difference scheme in space are used.

For conjugate heat transfer modelling, to evaluate the discretized temperature equation diffusion coefficients Γ, harmonic means are used. If $\Gamma = [(\mu/Pr) + (\mu_{\mathrm{T}}/Pr_{\mathrm{T}})]$ then for a control volume face located exactly half way between nodes i, j, k and i, $j+1$, k the diffusion coefficient at the control volume face takes the form

$$\Gamma = \frac{2\Gamma_{i,j,k}\Gamma_{i,j+1,k}}{\Gamma_{i,j,k} + \Gamma_{i,j+1,k}} \tag{13}$$

Similar expressions can be used for other faces.

To reduce excessive near wall turbulence kinetic energy levels, an under-relaxation procedure is tested. The under-relaxation procedure is applied when solving the momentum equations and the temperature equation by updating the velocity and temperature as follows:

$$\phi = (1 - \lambda)\phi^{\text{old}} + \lambda\phi^{\text{new}} \tag{14}$$

where λ is the relaxation factor. Note, the 'old' and 'new' superscripts refer to time levels and are not used in the iterative sense. In the RANS zone $\lambda = 0.1$. The same linear weighting function used for the length scales and constants i.e. Equations (9) and (10) are employed to obtain the relaxation factors in the transitional zone.

The use of larger near wall time steps is also considered as a means of reducing near wall turbulence levels. Again, Equations (9) and (10) are employed to blend the larger near wall time steps to the smaller LES region steps. To improve stability, in the large time step zone the dissipative but stable hybrid (for cell Peclet number greater than two first order upwinding is used) convective scheme is used.

For the conjugate heat transfer problem, due to the large ratio of the thermal diffusivities for the fluid and the solid, it is found that the heat transfer process develops slowly during the calculation. In order to solve this numerical stiffness, three techniques were tested. One approach is that the temperature equation is not solved until the velocity field has been established. The velocity field is then frozen and just the temperature equation solved until the temperature field has developed. After this, the velocity and temperature field are solved together. This is necessary since the temperature depends on the fluctuating velocity of the fluid. The second technique involves a gradual increase in the ratio of the thermal diffusivities. The third uses the fully implicit time scheme and hybrid spatial scheme for the temperature equation. This allows larger initial time steps when solving the temperature equation. All these techniques have been found effective in reducing the computing costs, especially the second.

3. RESULTS AND DISCUSSION

3.1. Plane channel flow simulation

The new hybrid approach is first applied to a plane channel flow with a Reynolds number $Re_\tau = \rho u_\tau \delta/\mu = 1050$. The (x, y, z) domain size of $2\pi \times 2 \times \pi$ is discretized with a $33 \times 65 \times 33$ grid. The grid expansion factor in the cross channel y direction is 1.15. This ensures y^+ at the first off-wall nodes is around 1. The grid points in the streamwise and spanwise directions are uniformly distributed. This results in the grid spacing $\Delta x^+ \approx 200$ and $\Delta z^+ \approx 100$, which is obviously too big for an accurate LES simulation. Hence, near wall modelling is necessary.

To define the 'DES buffer/transitional layer' $y_A^+ = 30$ and $y_B^+ = 60$ are chosen. Figure 2 shows the curves for the length scales l_ε and l_μ, and changes of the length scales when the linear weighting function is employed. Investigations show the RANS length scales naturally intersect the LES at $y^+ \approx 18$ and 30 for l_ε and l_μ, respectively. This indicates that, at interfaces beyond these two locations, the RANS length scales are larger than the LES. Obviously, without smoothing technique or local length scale modifications, length scale discontinuities are inevitable. Figure 3 compares the law of the wall obtained with and without smoothing and also using the new hybrid LES/RANS approach with a linear weighting function. The symbols show the 'benchmark' LES data of Piomelli [31]. The figure shows that without

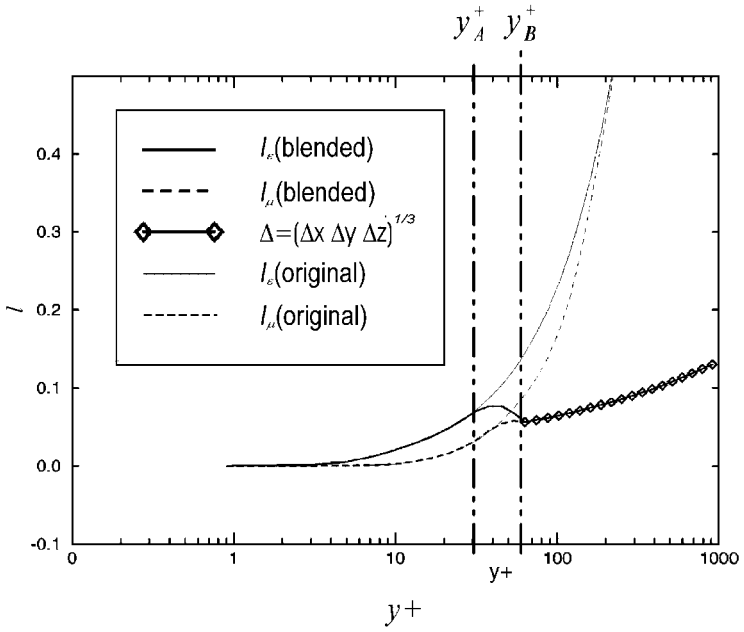

Figure 2. Length scales modification.

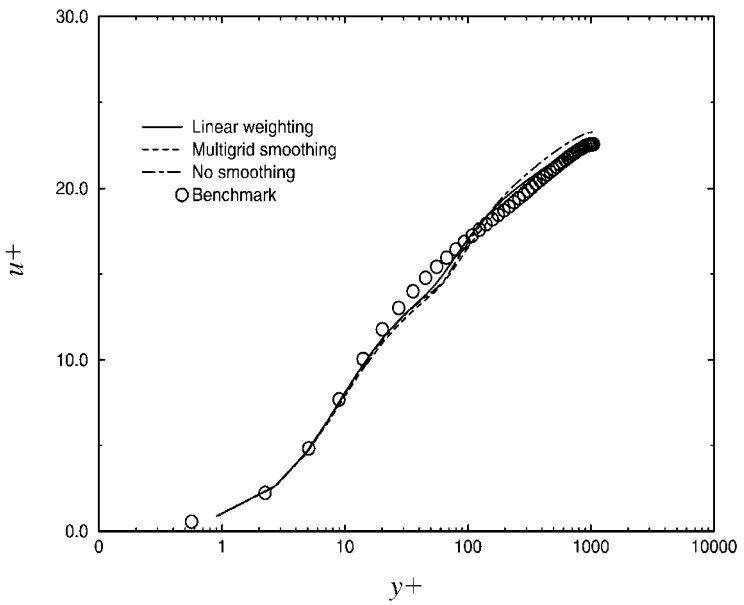

Figure 3. Law of the wall compared with results of Reference [18].

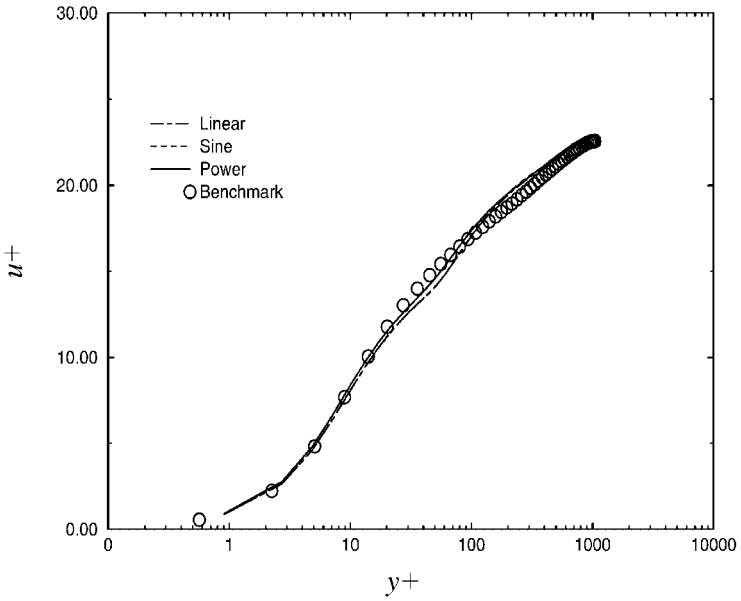

Figure 4. Wall laws for different weighting functions.

length scale smoothing, a kink occurs in the velocity profile. Figure 4 compares the results obtained using the linear, $\sin^2(\pi\xi/2)$ and $\xi^{1/3}$ weighting function. The function $\sin^2(\pi\xi/2)$ gives the smoothest transition between the RANS and LES length scales. However, $\xi^{1/3}$ gives the most accurate velocity profile. Nonetheless, expect for the slight velocity profile kink, evident around the transitional zone, the law of the wall is satisfactory for all three functions.

Numerical simulations show that when the RANS/LES interface tends towards the buffer layer, the RANS zone shows significant unsteadiness [18, 20]. This is because the resolved LES scales buffet the 'RANS' zone. Since the latter is calibrated to give correct near wall turbulence levels, the additional resolved scales create a near wall turbulence energy level surplus [18–20]. The ξ^n $(0<n<1)$ profiles give the lowest integrated near wall modelled l distribution. This might help alleviate the excessive near wall energy problem. However, reducing the modelled μ_T distribution reduces resolved scale damping and so this might not be the case. The near wall turbulence energy surplus can be seen from Figure 5. For illustrative purposes, $y_A^+ = 35$ and $y_B^+ = 220$ are chosen. These values correspond to $y_A/\delta = 0.033$ and $y_B/\delta = 0.21$. Again, the symbols give the benchmark data. Clearly, the sum of the modelled and resolved flow components, represented by dash lines, is too high.

Figure 6 shows that, by using the under-relaxation equation (14) in the RANS and transitional zones, the resolved kinetic energy has been reduced to the level of benchmark data. Work is still needed to make the total kinetic energy curve smoother. Also, improvements in turbulence energy level tend to deteriorate the law of the wall.

Figure 7 shows the velocity time history in the RANS, transitional and LES zones. Undesirable velocity fluctuations in the RANS and transitional zones are clear. Figure 8 shows the

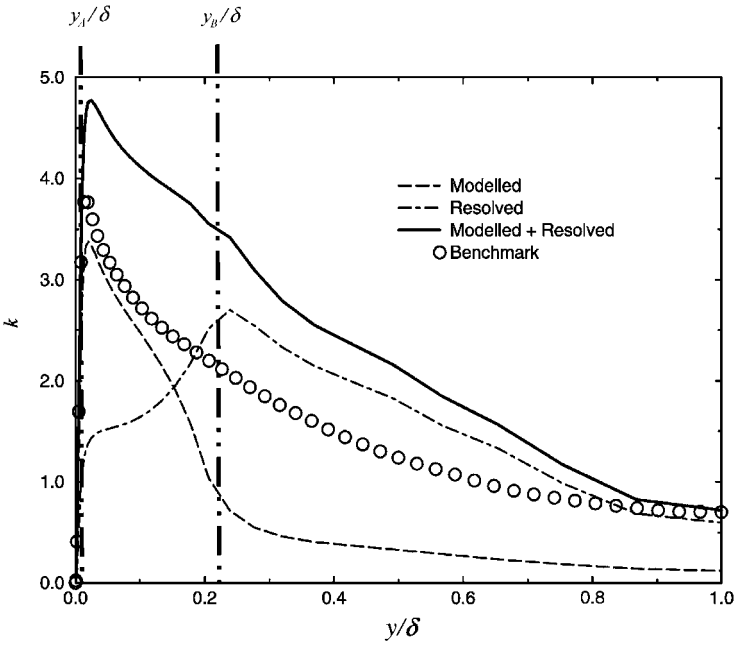

Figure 5. Kinetic energy distributions.

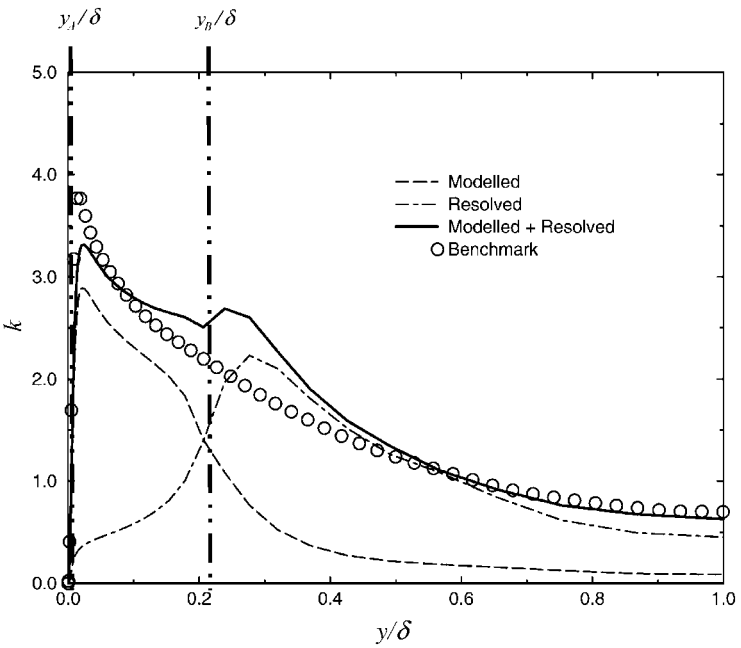

Figure 6. Kinetic energy level when using under-relaxation.

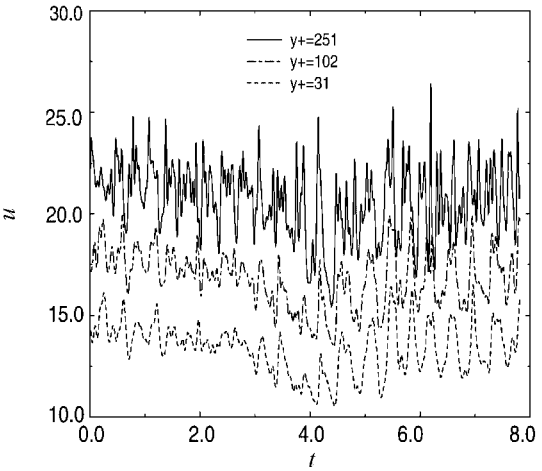

Figure 7. Time history of the velocity near the wall.

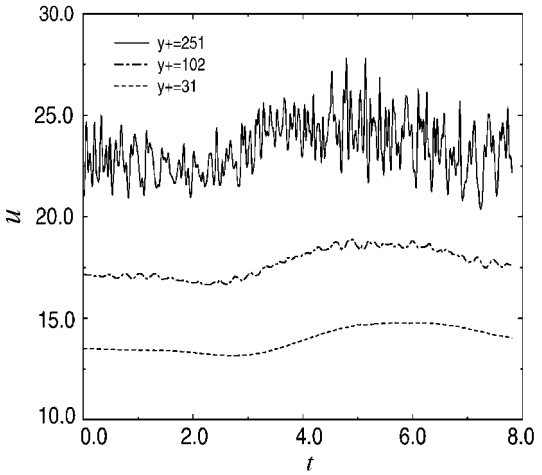

Figure 8. Time history of the velocity near the wall when using under-relaxation.

velocity time history after using under-relaxation. As can be seen, the velocity fluctuations in the RANS transitional zones have been severely damped. This is not just desirable for ensuring sensible total turbulence levels. If the 'RANS' zone resolved time scales are not much greater than the time scales implied by the model, the solution cannot be considered a theoretically correct URANS.

The modelled time scale t_{mod} in the RANS region can be estimated as $l/k^{1/2}$. For the current simulations, this gives at $y^+ = 60$ $t_{\mathrm{mod}} \approx 0.05$ s. Numerical investigations show that increasing time step Δt by a factor of 10 in the RANS zone can also give a minor beneficial reduction in the resolved near wall turbulence. However, approximately a factor of 1000 increase in Δt

would be required (i.e. produce a three orders of magnitude separation in the modelled and resolved time scales) for near wall URANS theoretical correctness.

3.2. Surface mounted cube flow simulation

The new hybrid LES/RANS approach has also been applied to the flow over a matrix of surface mounted cubes (see Figure 9). This configuration is of significant importance in many areas including wind engineering and electronics cooling [24]. It has been used for validation purposes by many groups in the 8th ERCOFTAC/IAHR/COST Workshop on refined turbulence modelling [25, 26, 32]. The results obtained using RANS with different turbulence models, LES and coarse grid DNS were compared. Nevertheless, the RANS results presented were unsatisfactory. Hence, this case provides a solid database for validating the newly developed hybrid LES/RANS approach.

The configuration consists a matrix of cubes of height $H = 15\,\text{mm}$ which are placed on the wall of a two dimensional channel of height $3.4H$. The configuration is sketched in Figure 9. The distance between the cubes is $4H$. The heated cube is made of a copper core covered with a thin layer of epoxy. The thickness of the epoxy is $0.1H$. Inside the copper core is an electric heater keeping the copper core at a constant temperature of 75°C. The Reynolds number based on channel height is $Re = 13,000$. This is equivalent to an inflow bulk velocity $U_0 = 3.86\,\text{m/s}$ (based on properties given later) rendering the mass flow rate per sub channel $\dot{m} = 13.70 \times 10^{-3}\,\text{kg/s}$.

In order to make the simulation results more comparable to other researchers' work, most of parameters used in the calculations are chosen to be consistent with those stated in Reference [24]. For clarity and completeness, these parameters will be repeated here. The temperature of the incoming flow is fixed to the reference value $T_{\text{ref}} = 20°\text{C}$. The material properties are listed in Table I.

The hybrid LES/RANS simulations are performed with a grid which has 421 875 points (each co-ordinate direction has 75 grid points with 7 nodes in the epoxy). The vertical

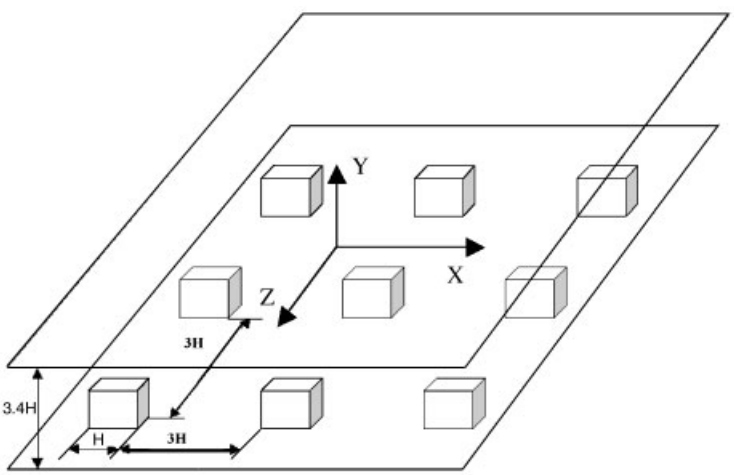

Figure 9. Configuration for the matrix of cubes.

Table I. The properties of air and epoxy.

	Air	Epoxy
Density ρ (kg/m^3)	1.16	1150.0
Viscosity μ (m^2/s)	41.818×10^{-5}	—
Thermal conductivity λ (kgm/s^{3}K)	0.0257	0.236
Specific heat Cp (m^2/s^{2}K)	1007.0	1668.5

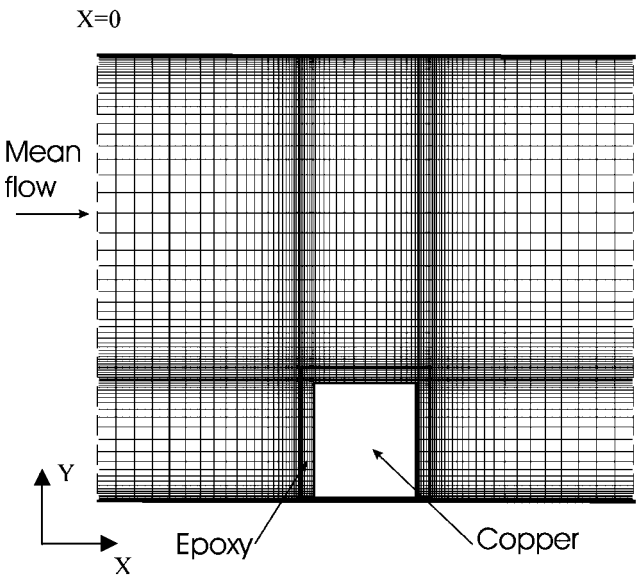

Figure 10. The grid in the symmetrical plane used for hybrid LES/RANS calculation.

symmetry plane grid is shown in Figure 10. The calculation domain consists of a sub-channel unit of dimension $4H \times 4H \times 3.4H$ encompassing the cube which is placed at the domain centre. The x and z axes are taken in the streamwise and the spanwise directions, respectively, and the y axis denotes the vertical direction.

As can be seen, the grid points are stretched towards all solid walls and the interfaces between the epoxy and the copper core of the cube. As in the LES simulation of Reference [24], the normal distances at the first off wall nodes are slightly smaller than $0.006H$. Numerical simulations show that for this grid, y^+ is around 1–2 on most walls, except around the corners, where y^+ can be slightly larger. An LES calculation is also performed with a grid of about 1.3 million grid points (each direction having 109 points with 9 nodes in the epoxy). The normal distances at first off wall nodes are set to $0.004H$. This results in a $y^+ \approx 1$ at all first off-wall grid nodes.

Same as in the plane channel case, $y_A^+ = 30$ and $y_B^+ = 60$ are chosen to define the 'DES buffer/transitional layer'. The linear weighting function is used for connecting the RANS and

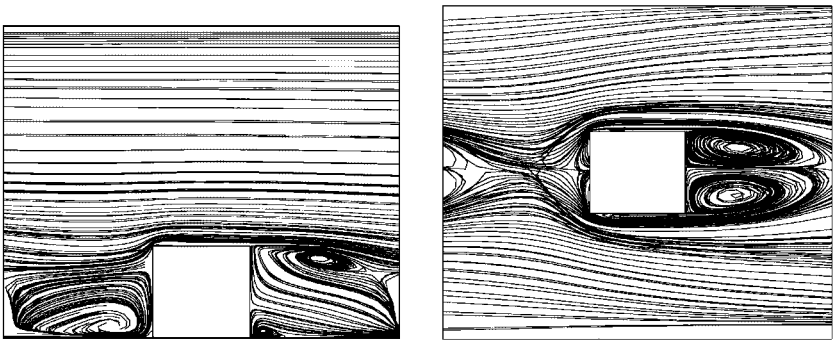

Figure 11. Hybrid LES/RANS time averaged streamlines.

LES zones. The hybrid LES/RANS and LES calculations are started either from fine grid URANS solutions using the k–l one equation turbulence model or by overlaying coarse grid LES/RANS or LES solutions. It is found that this can significantly reduce the computing costs.

Periodic boundary conditions are applied for the velocity in both the streamwise and spanwise directions. The temperature of the incoming fluid is set to the fixed reference value. At the domain outlet, the normal derivative of temperature is assumed to equal zero.

Figures 11(a) and 11(b) show the time-averaged hybrid LES/RANS streamlines in the vertical symmetry plane $z/H = 2.0$ and a horizontal plane at $y/H = 0.15$, respectively. Figure 11(a) shows that two re-circulation zones are formed at the foot of the cube front and rear, respectively. A stagnation point can be clearly identified in the front face near the top of the cube. Figure 11(b) shows that a horseshoe shape vortex is formed in front of the cube. Two small re-circulation regions on the sidewalls can also be detected. Behind the cube, two contra-rotating vortices can clearly be seen. Figure 12 gives three-dimensional top, side and perspective view of the time averaged streamlines, in which the main features of the flow structures are revealed. It can be seen that the streamlines pass the sidewalls and they are sucked into the two upward contra-rotating vortices. These two upward vortices meet at the top shear layer and leave the domain, forming an arch shaped vortex in the wake.

Figure 13 compares of the time averaged, nominally streamwise, velocity profiles in the vertical symmetry plane at $x/H = 1.2, 1.8, 2.8, 3.2$ and 3.8, respectively. The results suggest that the hybrid LES/RANS scheme simulates the re-circulation flow much better than the RANS. The hybrid LES/RANS results match the experimental data well and have comparable accuracy to the LES. The RANS results of Reference [26] use the Launder–Sharma low Reynolds number k–ε model. They are chosen because it is a unique RANS solution which includes temperature data. Figures 14 and 15 show the Reynolds stresses profiles of the $u'u'/U_0^2$ and $w'w'/U_0^2$ components in the vertical symmetry plane at $x/H = 1.2, 1.8, 2.8, 3.2$ and 3.8, respectively. It is interesting to note that the values of Reynolds stresses in all these profiles obtained with the hybrid LES/RANS scheme are close to that of the LES. On the contrary, the Reynolds stresses for the RANS results appear to be significantly overestimated. Figure 16 compares the modelled and resolved stress for both LES and hybrid LES/RANS.

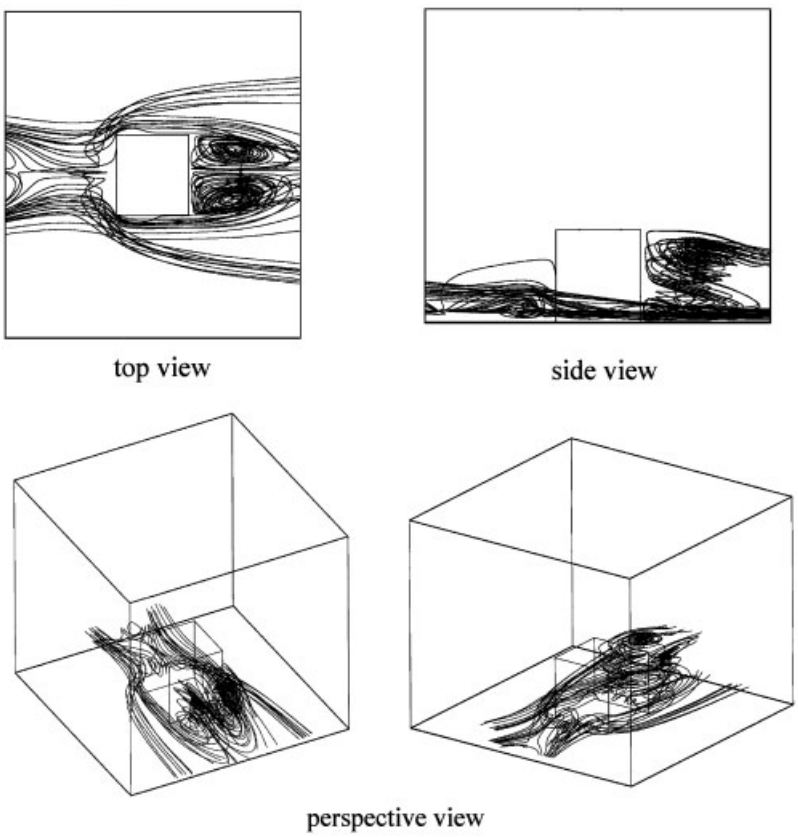

Figure 12. Hybrid LES/RANS time averaged streamlines.

The profiles are in the same location as for Figure 15. As would be expected, for the hybrid LES/RANS, near walls the modelled turbulence is higher than that for the LES. Consequently, the resolved energy is lower. For both approaches, away from walls, the modelled energy is a small fraction (around 10% for LES and 20% for hybrid LES/RANS) of the resolved. Figure 17 compares time averaged streamwise velocity component distributions in the horizontal plane half way up the cube at $x/H = 1.2, 1.8, 2.8, 3.2$ and 3.8, respectively. It shows that hybrid LES/RANS and LES results are much better than those from RANS, especially in the wake region behind the cube, where the arch shaped vortex is formed. The profiles suggest that the position of the arch shaped vortex is better predicted in the hybrid LES/RANS and LES simulations. Compared to the RANS [26] and the LES results, those obtained using the hybrid LES/RANS scheme are encouraging. With one-third grid points used for the LES calculation, the hybrid LES/RANS gives results almost comparable to the LES. On the contrary, the RANS solution behaves very differently. In some regions, especially in those behind the cube, RANS gives the incorrect trends. The RANS simulation also performs badly for the Reynolds stresses predictions.

One of the important goals of this paper is to investigate the capability of the hybrid LES/RANS scheme when predicting heat transfer. The heat transfer coefficients at three

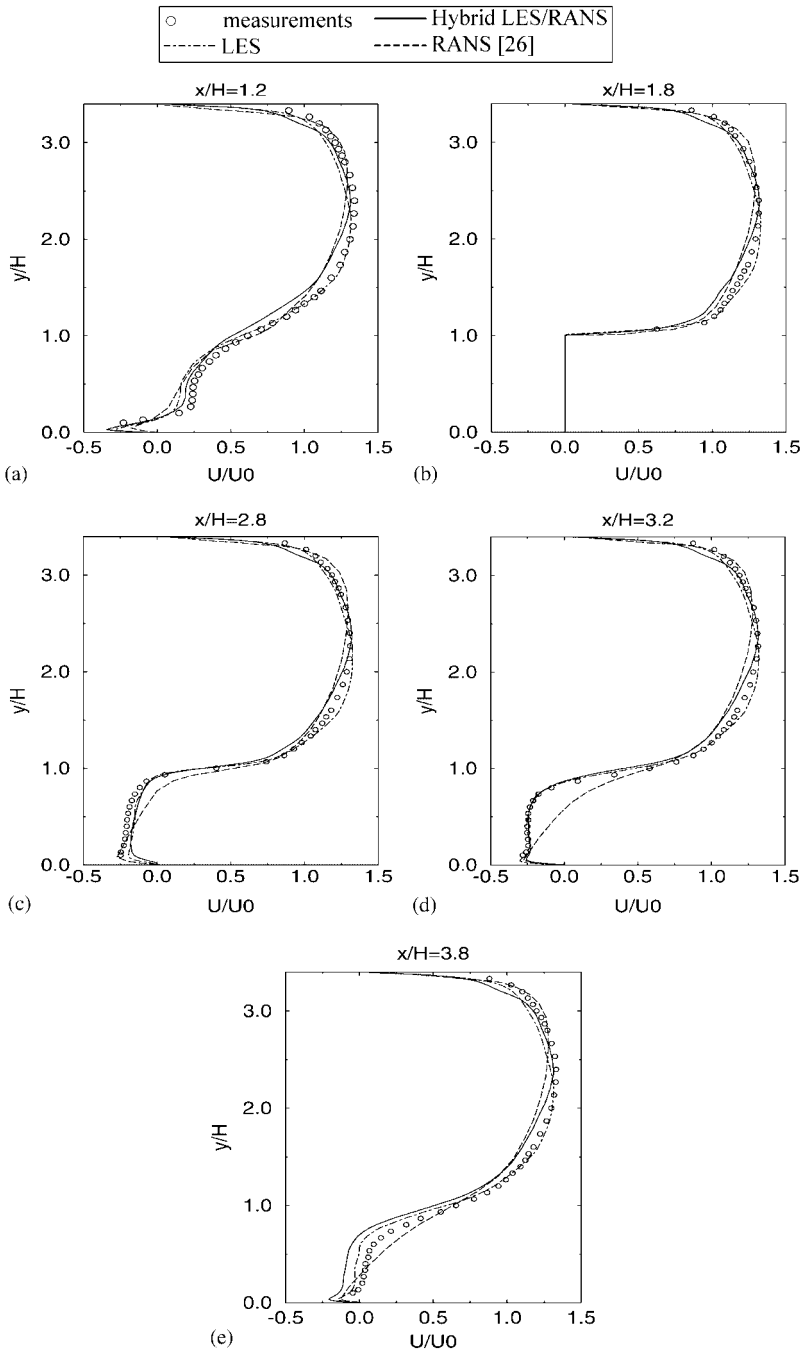

Figure 13. Comparisons of mean velocity profiles.

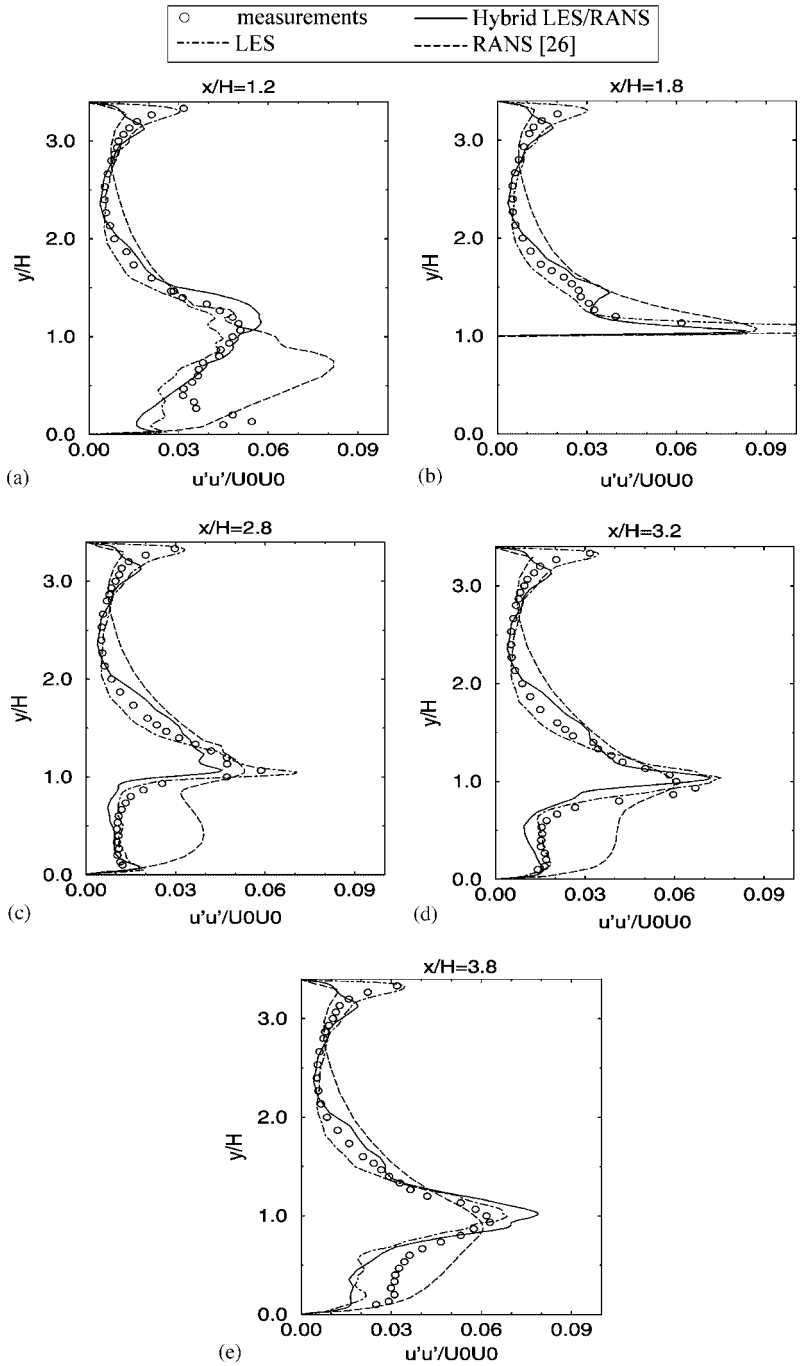

Figure 14. Comparisons of Reynolds stress profiles.

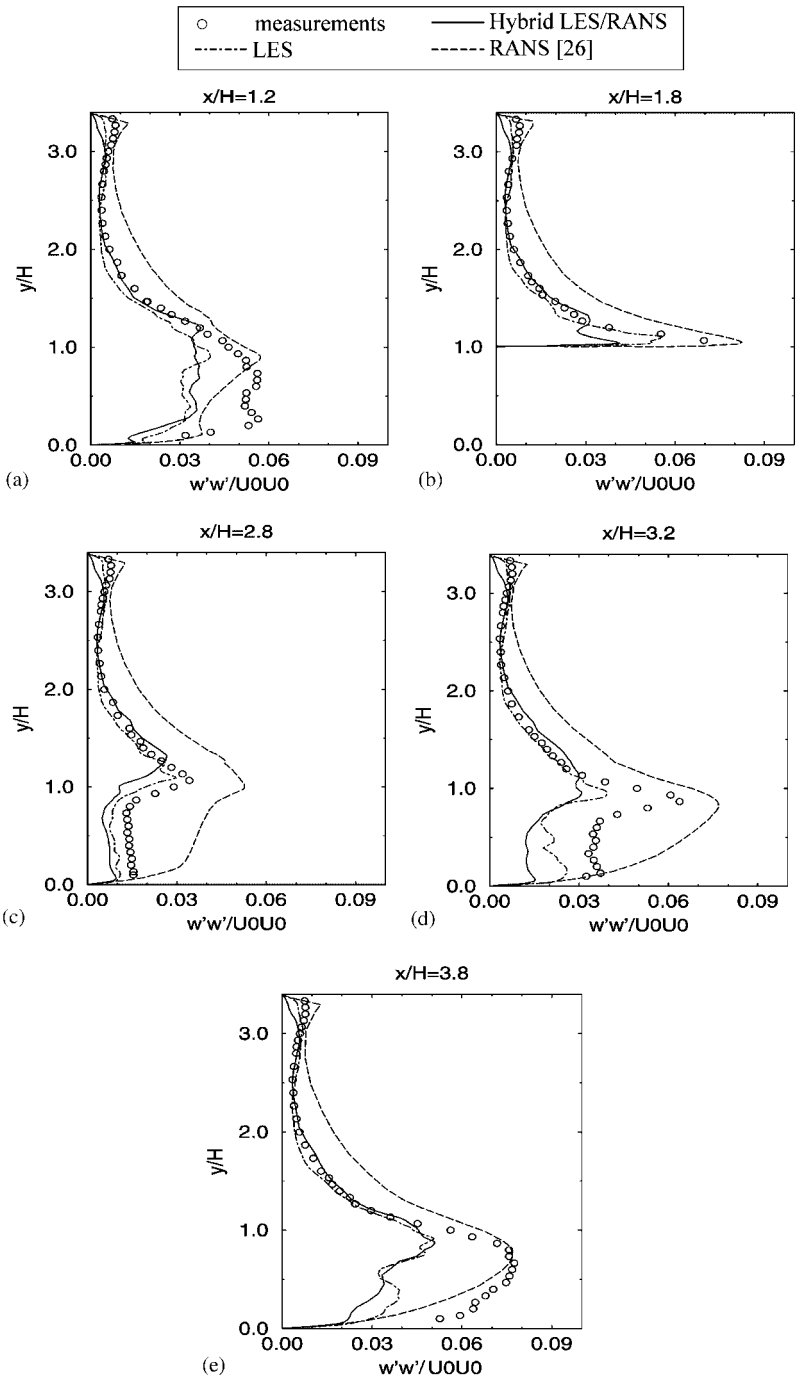

Figure 15. Comparisons of Reynolds stress profiles.

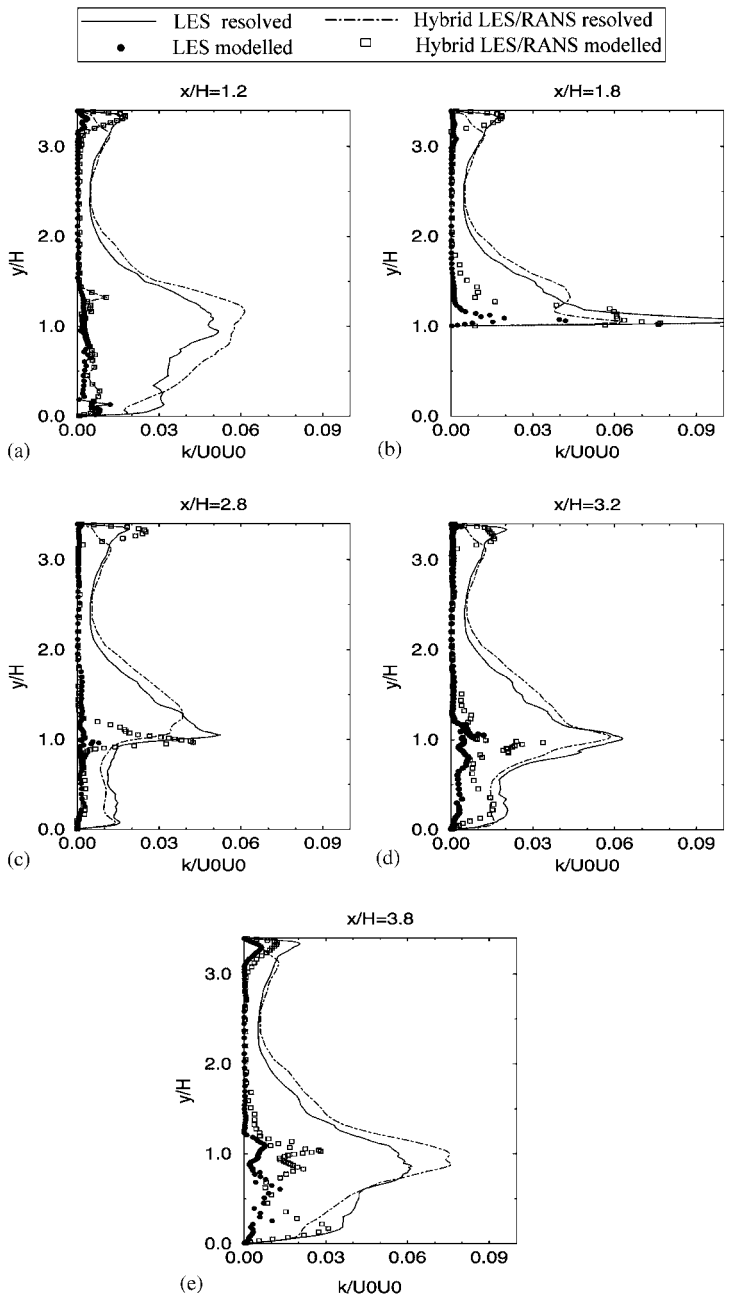

Figure 16. Comparisons of kinetic energy profiles.

profiles in horizontal and vertical planes have been examined. Figures 18(a) and 18(b) show schematically the positions in the horizontal and vertical planes where the heat transfer coefficients are examined.

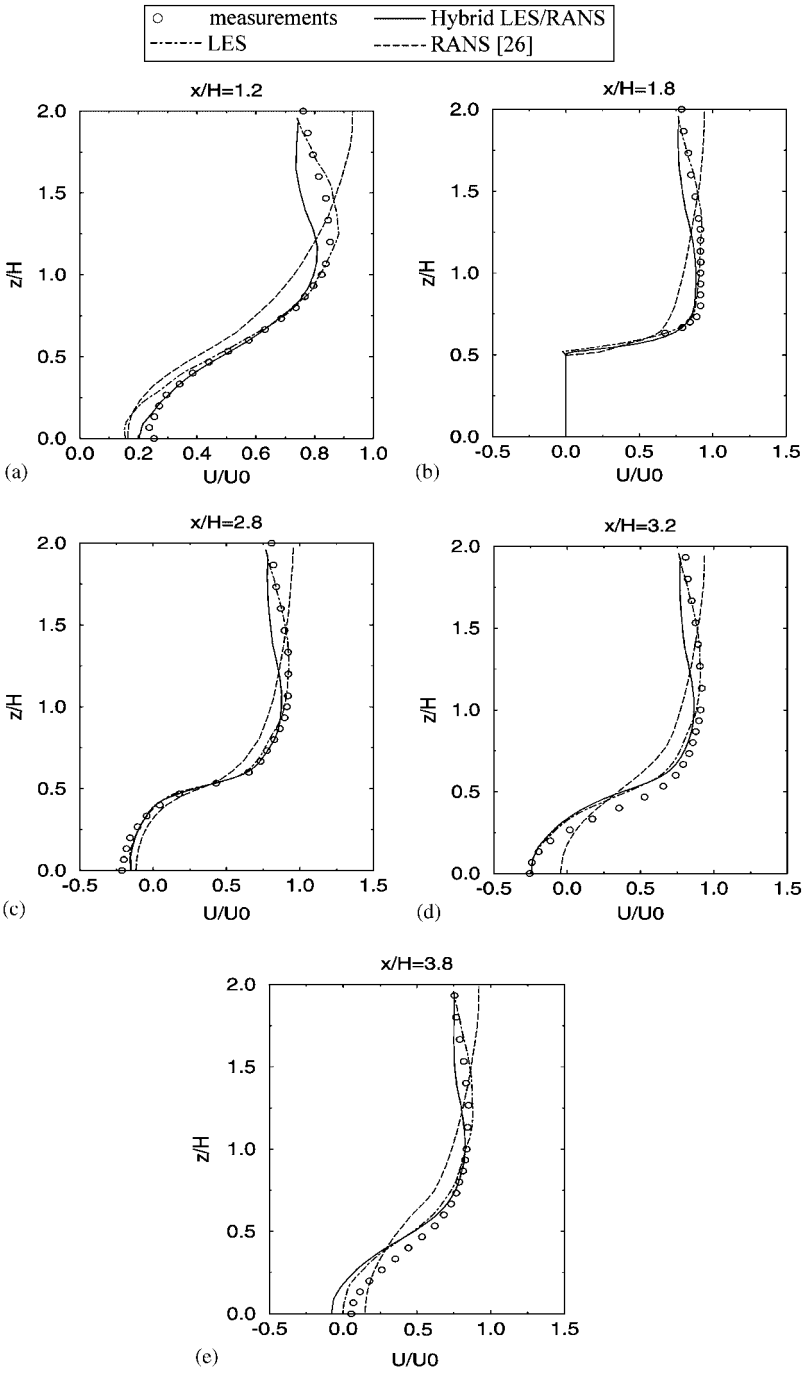

Figure 17. Comparisons of mean velocity profiles.

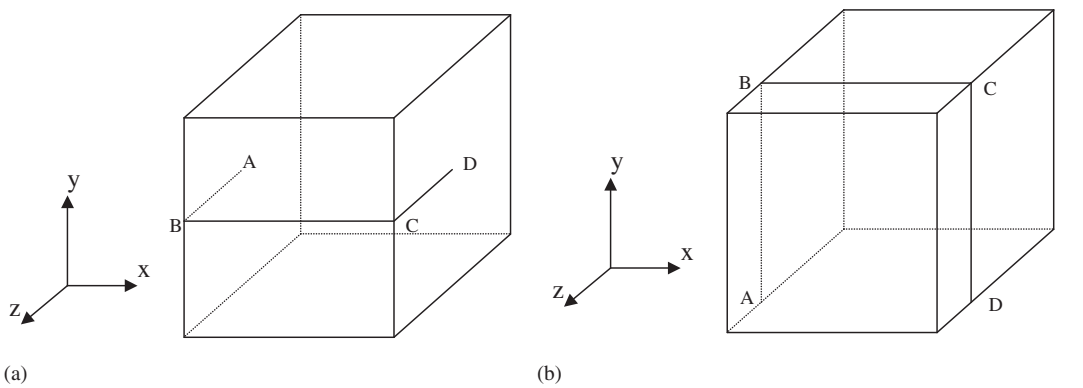

Figure 18. Surface temperature path lines.

Figures 19(a)–19(c) compare the surface heat transfer coefficients in the horizontal planes at $y/H = 0.25$, 0.52 and 0.75. Compared to the RANS [26], the results from the LES and hybrid LES/RANS approaches are overall better. The RANS solution is especially poor at the sidewalls. Encouragingly, the hybrid LES/RANS results are quite close to that from LES simulation.

Figures 19(d)–19(f) compare the surface heat transfer coefficients in the vertical planes at $z/H = 2.0$, 2.18 and 2.32. It should be noted that $z = 2.0$ is the symmetry plane. Accuracy improvements on the top surface (corner B–C) can be identified. Again, the hybrid LES/RANS results follow the LES trends, although understandably that the hybrid scheme results are slightly worse than those for the LES. It should be mentioned here that the discrepancies of the results near the channel floor (front corner A and rear corner D) are probably because the heat loss of the epoxy layer through the base wall are not well modelled [24]. In our simulation, the temperatures at floor adjacent nodes inside epoxy are set approximately to the averaged measured value, i.e. $T = 46°C$.

4. CONCLUSIONS

In this paper, to bridge RANS and LES zones, a controllable transitional zone is introduced. To obtain a smooth variation of the length scales and transitional zone parameters, different weighting functions are proposed. The compatibility of a k–l based hybrid LES/RANS method is improved. The new approach is tested for a plane channel flow and the flow over a matrix of surface mounted cubes. The later is a conjugate heat transfer problem. Numerical tests show that, compared to a RANS simulation for the flow with large scale unsteadiness, the proposed hybrid LES/RANS scheme performs well and is effective at improving the predicted heat transfer.

To improve near wall turbulence levels and ensure URANS theoretical correctness, the use of velocity under-relaxation and time step filtering is explored. The former approach is found more effective. However, it is not found possible to simultaneously match the mean and instantaneous benchmark data in the near wall region.

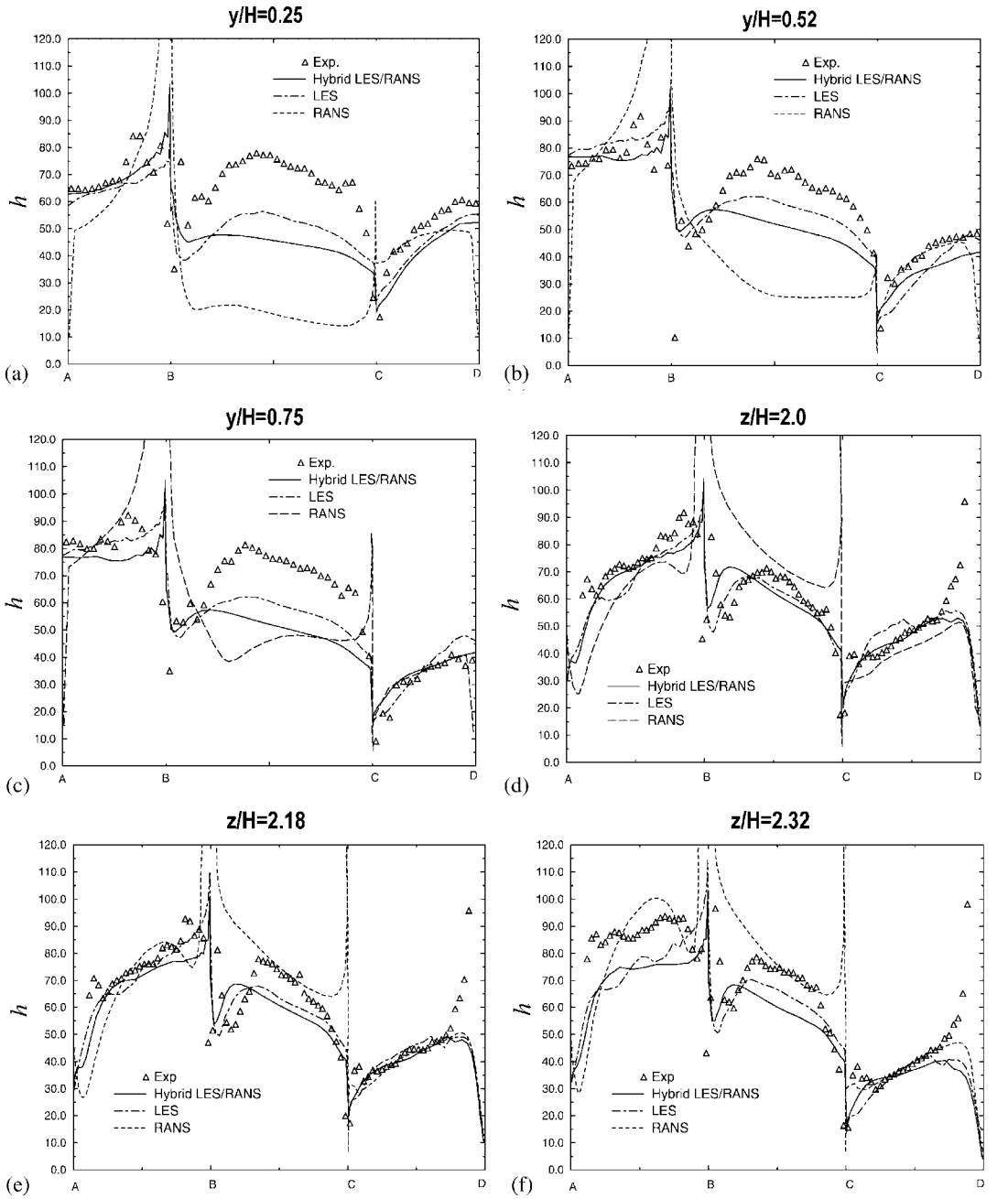

Figure 19. Heat transfer coefficients in a cube matrix.

ACKNOWLEDGEMENT

Engineering and Physical Sciences Research Council (EPSRC) funding under grant number GR/N399 20/01 is gratefully acknowledged.

REFERENCES

1. Piomelli U, Balaras E. Wall-layer models for large-eddy simulations. *Annual Review of Fluid Mechanics* 2002; **34**:349–374.
2. Spalart PR, Jou WH, Strelets M, Allmaras SR. Comments on the feasibility of LES for wings, and on a hybrid RANS/LES approach. *First AFOSR International Conference on DNS/LES*, 1997; Also in *Advances in DNS/LES*, Liu C, Liu Z (eds). Greyden Press, Louisiana Tech University: Ruston, LA, 1997; 137–147.
3. Piomelli U, Balaras E, Squires KD, Spalart PR. Interaction of the inner and outer layers in large-eddy simulations with wall-layer models. In *Engineering Turbulence Modelling and Experiments*, vol. 5, Rodi W, Fueyo N (eds). Elsevier Science Ltd: New York, 2002; 307–316.
4. Schumann U. Subgrid scale model for finite difference simulations of turbulent flows in plane channels and annuli. *Journal of Computational Physics* 1975; **18**:376–404.
5. Piomelli U, Ferziger J, Moin P. New approximate boundary conditions for large eddy simulations. *Physics of Fluids A* 1989; **1**:1061–1068.
6. Werner H, Wengle H. Large-eddy simulation of turbulent flow over and around a cube in a plane channel. In *Turbulent Shear Flows*, vol. 8. Springer-Verlag: Berlin, 1991; 155–168.
7. Baralas E, Benocci C. Subgrid-scale models in finite-difference simulations of complex wall bounded flows. *AGARD CP 551*. Neuilly-Sur-Seine: France, 1994; 2.1–2.5.
8. Cabot W, Moin P. Approximate wall boundary conditions in the large-eddy simulation of high Reynolds number flow. *Flow, Turbulence and Combustion* 1999; **63**:269–291.
9. Batten P, Goldberg U, Chakravarthy S. Sub-grid turbulence modelling for unsteady flow with acoustic resonance. *AIAA Paper* 2000-0473, 2000.
10. Batten P, Goldberg U, Chakravarthy S. LNS—an approach towards embedded LES. *AIAA Paper* 2002-0427, 2002.
11. Batten P, Goldberg U, Chakravarthy S. Using synthetic turbulence to interface RANS and LES. *41st Aerospace Sciences Meeting & Exhibit*, *AIAA Paper* 2003-0081, 2003.
12. Nikitin NV, Nicoud F, Wasistho B, Squires KD, Spalart PR. An approach to wall modelling in large eddy simulations. *Physics of Fluids* 2000; **12**:1629–1632.
13. Spalart PR. Strategies for turbulence modeling and simulations. *International Journal of Heat and Fluid Flow* 2000; **21**:252–263.
14. Strelets M. Detached eddy simulation of massively separated flows. *AIAA Paper* 2001-0879, 2001.
15. Davidson L, Peng SH. A hybrid LES-RANS model based on a one-equation SGS model and a two-equation k–ω model. *International Journal for Numerical Methods in Fluids* 2003; **43**:1003–1018.
16. Temmerman L, Leschziner MA, Hanjalic K. *A-priori* studies of a near-wall RANS model within a hybrid LES/RANS scheme. In *Engineering Turbulence Modelling and Experiments*, vol. 5, Rodi W, Fueyo N (eds). Elsevier Science Ltd: New York, 2002; 317–325.
17. Hamba F. An approach to hybrid RANS/LES calculation of channel flow. In *Engineering Turbulence Modelling and Experiments*, vol. 5, Rodi W, Fueyo N (eds). Elsevier Science Ltd: New York, 2002; 297–305.
18. Tucker PG, Davidson L. Zonal k–l based large eddy simulations. *Computers and Fluids* 2003; **33**:267–287.
19. Zhong B, Tucker PG, Liu Y. On a hybrid LES/RANS approach and its application to flow over a matrix of surface mounted cubes. *Proceeding of the 4th International Symposium on Turbulence, Heat and Mass Transfer*, 2003.
20. Temmerman L, Leschziner MA, Hanjalic K. A combined RANS-LES strategy with arbitrary interface location for near-wall flows. *Proceedings of the 3rd International Symposium on Turbulence and Shear Flow Phenomena* 2003; **III**:929–934.
21. Spezial CG. Turbulence modelling for time-dependent RANS and VLES: a review. *AIAA Journal* 1998; **36**:173–183.
22. Spalart PR, Allmaras SR. A one-equation turbulence model for aerodynamic flows. *30th Aerospace Sciences Meeting & Exhibit*, Reno, NV, *AIAA Paper* 92-0439, 1992.
23. Yoshizawa A. Bridging between eddy-viscosity-type and second order models using a two-scale DIA. *9th International Symposium on Turbulent Shear Flow* 1993; 23.1.1–23.1.6.
24. Niceno B, Dronkers ADT, Hanjalic K. Turbulent heat transfer from a multi-layered wall-mounted cube matrix: a large eddy simulation. *International Journal of Heat and Fluid Flow* 2002; **23**:173–185.
25. *Proceedings of the 8th ERCOFTAC/IAHR/COST Workshop on Refined Turbulence Modeling*, Report 127, Hellsten A, Rautaheimo P (eds), Helsinki University of Technology, Helsinki, Finland, ISBN 951-22-4772-0, ISSN 1455-7533, 1999.

26. Rautaheimo P, Siikonen T. Flow in a matrix of surface-mounted cubes—description of numerical methodology for test case 6.2. In *Proceedings of the 8th ERCOFTAC/IAHR/COST Workshop on Refined Turbulence Modeling*, Hellsten A, Rautaheimo P (eds). Report 127, Laboratory of Applied Thermodynamics, Espon, Helsinki University of Technology, Helsinki, Finland, 1999; 31–36.
27. Patankar SV, Liu CH, Sparrow EM. Fully developed flow and heat transfer in ducts having streamwise periodic variations of cross-sectional area. *ASME Journal of Heat Transfer* 1977; **99**:180–186.
28. Acharya S, Dutta S, Myrum TA, Baker RS. Periodically developed flow and heat transfer in a ribbed duct. *International Journal of Heat and Mass Transfer* 1993; **36**:2069–2082.
29. Wolfshtein M. The velocity and temperature distribution in one-dimensional flow with turbulence augmentation and pressure gradient. *International Journal of Heat and Mass Transfer* 1969; **12**:301–318.
30. Fureby C. Large eddy simulation of rearward-facing step flow. *AIAA Journal* 1999; **37**:1401–1411.
31. Piomelli U. High Reynolds number calculations using the dynamic subgrid-scale stress model. *Physics of Fluid* 1993; **5**:1484–1490.
32. Mathey F, Froehlich J, Rodi W. Flow in a matrix of surface-mounted cubes—test case 6.2: Description of numerical methodology. In *Proceedings*, *8th ERCOFTAC/IAHR/COST Workshop on Refined Turbulence Modeling*, Hellsten A, Rautaheimo P (eds). Report 127, Laboratory of Applied Thermodynamics, Espon, Helsinki University of Technology, Helsinki, Finland, 1999; 46–49.

